Novel Materials Based on Silicone–Acrylate Copolymer Networks

M. MAZUREK[1], D. J. KINNING[1], T. KINOSHITA[2]

[1] 3M/ATC, 3M Center, 201-4N-01, St. Paul, Minnesota 55144

[2] Takumi Kinoshita, Sumitomo/3M, Sagamihara, Japan

Received 1 February 2000; accepted 7 May 2000

ABSTRACT: This article presents a broad class of materials made by copolymerization of a family of telechelic free radically polymerizable siloxanes with various acrylate monomers that polymerize to form high T_g polymers. Films with properties ranging from strong elastomers to plastics have been obtained by UV-initiated bulk copolymerization of functional siloxanes dissolved in acrylate monomers (in the presence of a photoinitiator). The molecular weight of the functional siloxanes, the nature of functional endgroups, the choice of (meth)acrylate comonomer, and the siloxane/acrylate ratio all have a rather dramatic effect on the morphology, and thus, on the properties of the copolymeric networks. Physical properties of the materials, such as optical appearance and mechanical and transport properties are correlated with the unique morphologies observed by TEM studies. Unusual properties such as reversible whitening of some of the materials and low Poisson ratios have been attributed to the microcavitation observed when high T_g acrylate domains interfere with the network deformation. Networks composed of high T_g acrylates (major fraction) coreacted with elastomeric siloxanes can provide heat-shrinkable materials when they are elongated at temperatures higher than the T_g of the corresponding polyacrylates and quenched.
 J Appl Polym Sci 80: 159–180, 2001

Key words: polydimethylsiloxane; acrylate; interpenetrating polymer network; morphology; mechanical properties; optical properties

INTRODUCTION

The discovery of new synthetic methods enabling the preparation of high purity telechelic polydimethylsiloxane diamines[1] prompted our interest in difunctional siloxanes having free radically polymerizable end groups, as the starting materials for silicone elastomers. Indeed, high-purity silicone diamines served as the building blocks to develop a family of free radically curable materials, by means of simple reactions with capping reagents such as isocyanatoethylmethacrylate (IEM), vinyldimethylazlactone (VDM), isopropenyl dimethyl azlactone (IDM), and *m*-isopropenyl-α,α-dimethyl benzyl isocyanate (*m*-TMI) to give the various telechelic siloxanes shown in Figure 1. The reactive polydimethylsiloxanes thus formed are referred to as MethAcryloxyUrea Siloxane (MAUS), ACrylaMidoAmido Siloxane (ACMAS), MethACrylaMidoAmido Siloxane (MACMAS), and MethylStyrylUrea Siloxane (MeStUS), respectively. Functional siloxanes with molecular weights in the range of 5000 to 100,000 have been prepared and studied.[2,3] These siloxanes, having free radically polymerizable end groups, proved to be of great practical and theoretical interest.[4,5]

Correspondence to: M. Mazurek.

Journal of Applied Polymer Science, Vol. 80, 159–180 (2001)

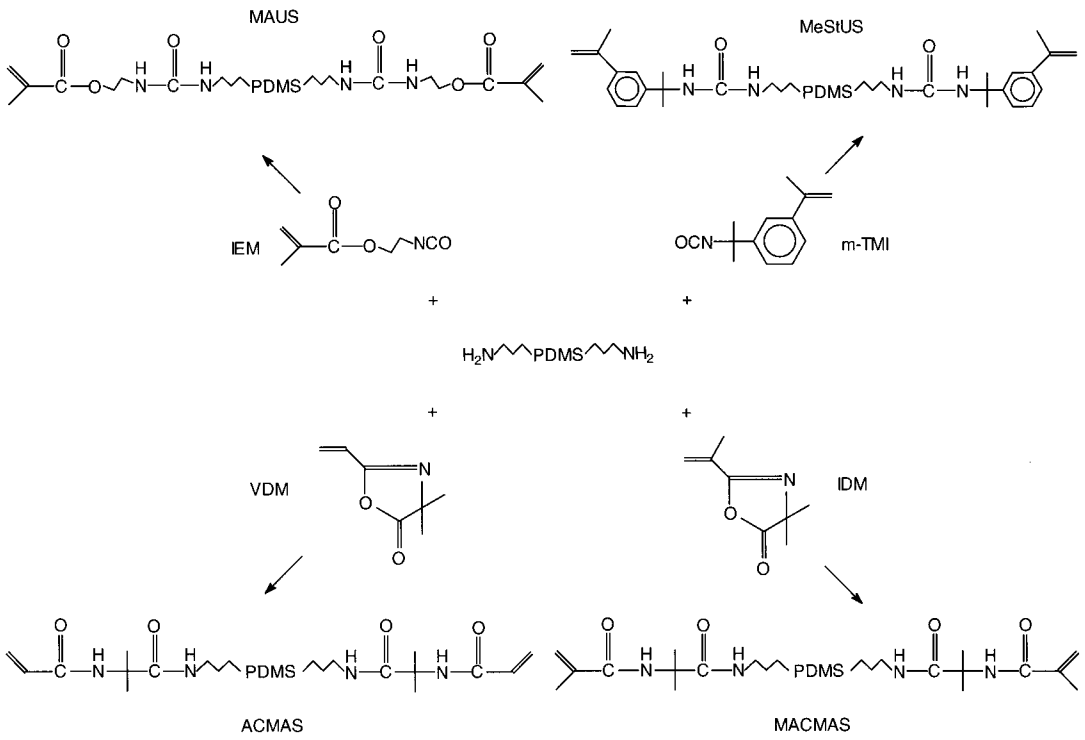

Figure 1 A family of free radically polymerizable telechelic siloxanes derived from α,ω-bis(aminopropyl)polydimethylsiloxanes.

Due to the polar nature of the hydrogen bonding end groups and the nonpolar nature of the polydimethylsiloxane chain, a transient network is formed wherein the polar end groups tend to associate with each other. The relative strength of the end group association for the various telechelic siloxanes is reflected in their viscosities, with higher viscosities seen in the case of the more strongly associating end groups (e.g., ACMAS and MeStUS).

Functional polymers that are easy to cure to elastomers are often referred to as "liquid rubbers." Indeed, by the exposure of telechelic siloxanes having free radically polymerizable end groups to low-intensity UV radiation (when the system contains photoinitiator), silicone elastomers with controlled properties can be obtained. The telechelic siloxanes can also be coreacted with a variety of acrylate and methacrylate monomers to form silicone–acrylate hybrid systems in which difunctional siloxanes function as polymeric crosslinkers. Depending on the composition, such copolymeric networks may have the properties of plastics, elastomers, pressure sensitive adhesives, etc. Some of the materials of this group have been described previously.[6]

There is a significant body of literature concerning silicone-based interpenetrating polymer networks (IPNs).[7–17] In the broadest sense, copolymeric networks can be considered to be a type of IPN. They are then referred to as graft, or joined IPNs.[18] Although hybrid networks composed of free radically polymerizable siloxanes and acrylates are known in the patent and trade literature,[6,19–26] there are very few articles describing this class of materials. Cooper et al.[27] prepared a series of UV-cured silicone–acrylate networks made from 1700 to 3700 molecular weight methacryloxyurea siloxanes and various reactive diluents (e.g., acrylate and methacrylate monomers). The networks were examined by stress–strain testing, dynamic mechanical measurements, and differential scanning calorimetry, which indicated that the networks possessed a two-phase morphology, although all samples were transparent. The aim of the present article is to describe the unique microphase-separated morphologies and physical properties of silicone–acrylate hybrid networks formed by the copolymerization of telechelic siloxanes with (meth)acrylate monomers (e.g., isobornyl acrylate) able to form high T_g (above room temperature) homopolymers.

Emphasis will be given to the tailorability of such properties as optical appearance, mechanical properties, and heat shrinkability of the copolymer networks. The oxygen permeability of such networks will also be discussed.

EXPERIMENTAL

Reactants

All reactants were used as received from the vendors.

Synthesis of Telechelic Siloxanes

Amine-Functional Siloxane Iintermediates

Bis(3-aminopropyldimethyl) polydimethylsiloxanes (silicone diamines) were synthesized according to the procedure described by Leir et al.,[1] which provides highly difunctional silicone diamines. Number-average molecular weights of the silicone diamines were determined by acid titration with 0.1 *N* HCl, using bromophenol blue as an indicator. GPC analysis of the silicone diamines indicated a normal molecular weight distribution with polydispersities of about 2.0.

Synthesis of ACMAS

Polydimethylsiloxanes having acrylamidoamido end groups were prepared by first heating silicone diamine under vacuum (aspirator) to 100°C to decompose any traces of carbamates, which could be formed by the reaction of the amine endgroups with CO_2. Then, 2 mol of vinyl dimethyl azlactone (VDM), purchased from SNPE, were added slowly to 1 mol of the silicone diamine at room temperature, while the reaction mixture was being stirred. An increase in viscosity was observed in all cases, but it was especially evident for lower molecular weight materials.

Synthesis of MACMAS

Polydimethylsiloxanes having methacrylamidoamido end groups were made in the same manner as described for ACMAS, using isopropenyl dimethyl azlactone (IDM), purchased from SNPE. Viscosities of the resulting polymers were much lower than for the corresponding ACMAS samples.

Synthesis of MAUS

Polydimethylsiloxanes having methacryloxyurea end groups were made using the same procedure, by reacting silicone diamines with isocyanatoethyl methacrylate (IEM), purchased from Showa Rhodia. The reaction is exothermic; thus, in the case of lower molecular weight diamines it is advisable to add IEM slowly, and cool the reaction mixture, if needed.

Synthesis of MeStUS

Polydimethylsiloxanes having α-methylstyrylurea end groups were made by reacting silicone diamines with *m*-isopropenyl-α,α-dimethyl benzyl isocyanate (*m*-TMI), purchased from Cyanamid. A strong increase in viscosity was observed, especially in the case of lower molecular weight siloxanes.

Viscosity Measurements

The viscosities of the intermediate silicone diamines and the telechelic silicones, as a function of molecular weight, were measured at 25°C using a model RVTDV-II Brookfield viscometer. Spindle #21, 27, or 29 was used, depending on the viscosity of the sample.

Preparation of Silicone–Acrylate Copolymeric Networks

The polymerization mixtures were prepared by dissolving telechelic siloxanes in the acrylate monomers (purchased from Aldrich). Most of the monofunctional acrylic monomers, with the exception of some strongly polar monomers such as acrylic acid, are good solvents for siloxanes. Of the polar monomers, methacrylic acid is a good solvent for polydimethylsiloxanes. Darocur™ 1173 photoinitiator was then added to the solutions, at a concentration of 0.5 wt %. Such solutions have viscosities that permit the preparation of samples in film form by direct coating and radiation curing by the standard procedures. Most of the samples were prepared by either spreading a polymerizable solution between two polyester films to form a layer approximately 0.3 mm thick, or by filling a mold, with the thickness regulated by a spacer, using a syringe. The most preferred curing procedure involves UV-initiated polymerization between two polyester films. Sylvania blacklights with intensity of 2.5 mW/cm^2 were used as a source of UV radiation. In most cases a sufficient dose of radiation was of the order of 400–1000 mJ/cm^2 (10 to 20 min exposure). It was also demonstrated that medium pressure high-intensity UV lights could be utilized for curing the samples

between two PET films. In the case when high-intensity UV lights were used (samples marked as hiUV), the dose used for curing was of the order of 1000 mJ/cm^2.

Characterization of Silicone–Acrylate Copolymeric Networks

Several methods have been used to correlate the optical, mechanical, and transport properties of the silicone–acrylate hybrid networks with their composition and morphology. The most relevant information regarding the morphology has been obtained using transmission electron microscopy.

Transmission Electron Microscopy

Thin sections, approximately 500 Angstroms thick, for transmission electron microscopy studies, were obtained using a Reichert-Jung Ultracut E ultramicrotome equipped with a FC 4D cryoattachment. A diamond knife having a stainless steel boat was used. Sections were floated off onto *n*-propanol and picked up on 700 mesh copper grids. The knife temperature was kept at −100°C, while the sample temperature was kept at −130°C. A JEOL 100 CX microscope, operated at 100 kV, and calibrated with a 2160 lines/mm replica grating, was used to take the electron micrographs. The silicone phases appear dark in the micrographs without the need for staining.

Stress—Strain Curves

Mechanical testing was performed on an Instron Model 1122 tensile tester. Testing was performed according to a modification of ASTM D412-83. Samples were prepared according to Method B (cut ring specimens). Type 1 rings (5.1 cm circumference) were produced with a specially designed precision ring cutter. Modifications to the ASTM test procedure were as follows: (1) the crosshead speed was 12.7 cm/min rather than 50.8 cm/min; (2) the test fixture shafts (upper and lower jaw) both rotated at 30 rpm in the same direction in order to maintain uniform strain throughout the entire ring; (3) the thickness of the rings was 0.3–0.5 mm. The reported tensile moduli data are an average of at least two measurements (in most cases three measurements). Values of the stress and strain at break are reported for the sample having the highest stress at break in the series.

Swellability/Extractability

Some of the samples were analyzed for extent of swelling and percent extractables in THF. Small discs were cut from the film samples (15 mm diameter × 0.3 mm thickness), weighed, and submerged in solvent for 24 h. The swollen samples were weighed, to determine the percent swelling, and then dried and reweighed to detect the level of extractables.

Rheometrics

Dynamic-mechanical properties of a few select samples were characterized in shear mode using a Rheometrics RDA II rheometer in the temperature sweep mode (5°C/min) at a frequency of 1 Hz.

Further Deformation Studies

Some of the more unique features of these materials were revealed upon deformation of the samples (examples are given in Table I). To elucidate the underlying phenomena, some of the samples were examined using the two methods of deformation described in the following paragraphs.

The first method was used to determine the volume changes upon elongation. The corners of a 20 ×20-mm square area on the film sample (100 × 30 × 0.3 mm) were chosen and marked for easy measurements. The initial length and width between the marks were measured. In addition, the film thickness was measured at the four points corresponding to the marks, using a caliper gauge (±0.01 mm), and averaged. Measurements of the length, width, and thickness were made at different elongations, and used to calculate the volume of the sample as a function of elongation.

To characterize the maximum elongation at break, and to determine how the maximum elongation depends on the strain and thermal history of the material, some representative samples have also been submitted to a sequence of elongation and heating (above the T_g of the acrylate polymer) steps as follows. As described above, the corners of a 20 × 20-mm square area of the film were marked for easy measurement. The initial length and width between the marks were measured, and the thickness at the four points corresponding to the marks was measured and averaged using a caliper gauge. The sample was subsequently stretched at room temperature to near the maximum elongation (to avoid breaking) and fixed in a jig. The length and width between the marks, as well as the thickness, were remeasured. The stretched sample was then placed in

Table I General Characteristics of Siloxane/Acrylate Copolymer Networks

Acrylate	Siloxane	Siloxane/ Acrylate (w/w)	Appearance	Mechanical Characteristics
IBA	50 K ACMAS	10/90	white	brittle
		25/75	translucent/white	flexible plastic, whitens upon stretching with easy to feel "friction"
		50/50	bluish	elastomer
		75/25	clear	elastomer
IBA	5 K ACMAS	50/50	slightly bluish	plastic
	20 K ACMAS	50/50	slightly bluish	flexible plastic
	35 K ACMAS	50/50	slightly bluish	elastomer
	90 K ACMAS	50/50	bluish	elastomer
t-BuA	50 K ACMAS	25/75	translucent	flexible plastic, whitens upon stretching
		50/50	slightly bluish	elastomer
CHA	50 K ACMAS	25/75	translucent/white	elastomeric at room temperature; at 15°C becomes flexible plastic, whitens upon stretching
TMCHA	50 K ACMAS	25/75	translucent	flexible plastic, whitens upon stretching
MMA	50 K ACMAS	25/75	translucent	elastomeric, whitens upon stretching
MAA	50 K ACMAS	25/75	white	very brittle plastic
		50/50	white	cheesy plastic
IBA	50 K MeStUS	25/75	clear	plastic, irreversibly whitens upon bending
		50/50	clear	plastic, very little elasticity gained upon elongation
IBA	50 K MACMAS	25/75	translucent	flexible plastic, whitens upon stretching with easy to feel "friction"
		50/50	clear	elastomer
IBA	50 K MAUS	25/75	bluish	plastic, irreversibly whitens upon stretching, becomes elastomeric in whitened areas
		50/50	clear	plastic, gains elasticity at low elongation

IBA = isobornyl acrylate.
t-BuA = *t*-butyl acrylate.
CHA = cyclohexyl acrylate.
TMCHA = trimethyl cyclohexyl acrylate.
MMA = methyl methacrylate.
MAA = methacrylic acid.

an oven at 120°C (above the T_g of the acrylate domains) for 0.5 h to relax the stress. After cooling the sample in the stretched form and removing it from the jig, the dimensions of the sample changed very little (only a few percent elastic recovery). If the sample was further stretchable, at room temperature, after such a deformation and heat treatment cycle, then the procedure was repeated as many times as possible. The ultimate elongation of the sample at break (or near break) was then measured. Eventually, the sample was placed in an oven at 120°C, without being fixed in the jig, and the extent of heat-shrinkability or permanent deformation was noted.

Oxygen Permeability

The oxygen permeability was measured using a MOCON oxygen permeability tester. Depending on the composition of the network, the thickness of the films used for oxygen permeability testing ranged from about 0.25 to 2.5 mm.

RESULTS AND DISCUSSION

General Optical and Mechanical Characteristics

A broad family of materials has been prepared to study the effect of the different compositional variables on the general characteristics of the resulting copolymer networks. Telechelic siloxanes with different functionalities (MAUS, ACMAS, MACMAS, and MeStUS) and a range of molecular weights (M_n of 5000 to 100,000) were coreacted with several different (meth)acrylate monomers (isobornyl acrylate (IBA), cyclohexyl acrylate, trimethyl cyclohexyl acrylate, methyl methacrylate, methacrylic acid, *t*-butyl acrylate (*t*-BuA)) at different ratios of siloxane to acrylate. Re-

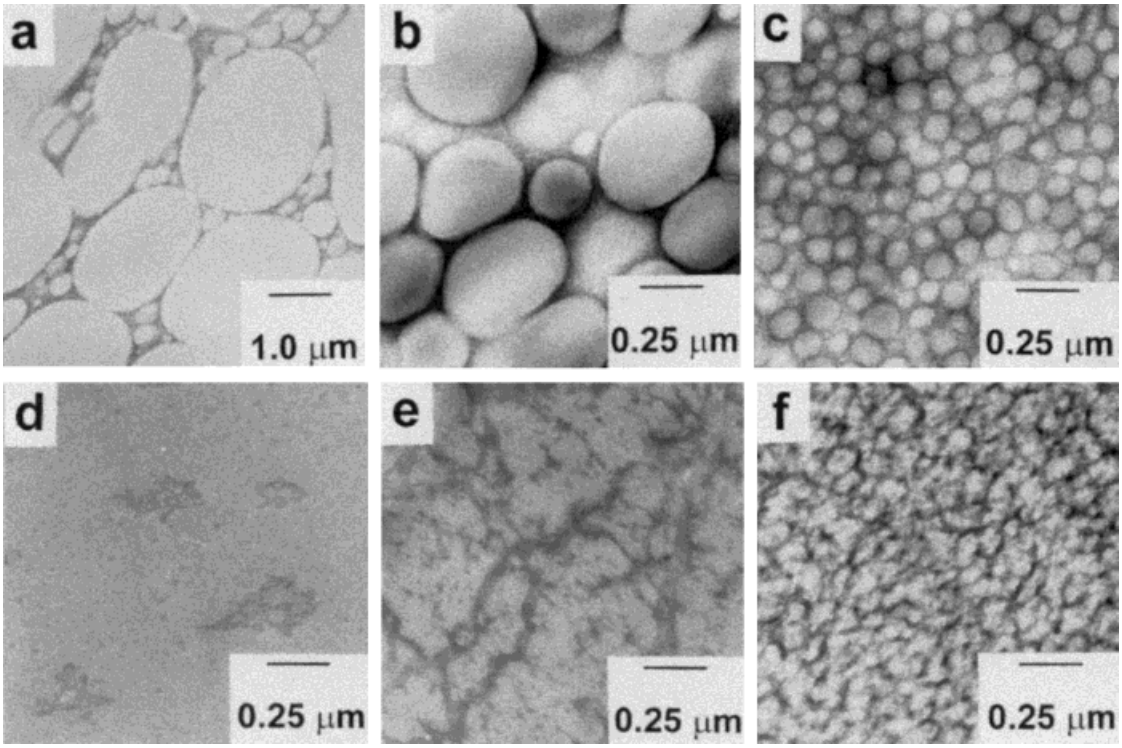

Figure 2 TEMs illustrating the effect of siloxane/acrylate ratio on the phase-separated morphology of 50K ACMAS/IBA networks: (a) 10/90, (b) 25/75, and (c) 50/50 (w/w), and 30K MAUS/IBA networks: (d) 5/95, (e) 15/85, and (f) 25/75 (w/w).

markably, in all cases a high degree of conversion of the (meth)acrylate monomers was observed, as judged by both the low residual odor and the low concentration of extractables, even though the polymerizations were done at temperatures much lower than the T_gs of the corresponding (meth)acrylate polymers. Some of the general optical and mechanical characteristic of the networks are described in Table I. It became apparent during the course of these initial screening experiments that materials with vastly different properties could be obtained from the same functional siloxane. For instance, copolymerization of 50K ACMAS with different acrylates at different siloxane/acrylate ratios can give transparent to white films, elastomers, or plastics, and reversibly or irreversibly changing optical characteristics upon stretching. In addition, changing the functional endgroup on the siloxane, the molecular weight of the siloxane, or the choice of (meth)acrylate comonomer can also change the network characteristics appreciably. The influence of these compositional variables on the appearance and physical characteristics of the resulting copolymer networks will be investigated more fully in subsequent sections of this article.

Description of TEMs

Effect of Silicone Content and Reactive Silicone End Group

Figure 2(a)–(c) shows electron micrographs of networks comprised of 50K ACMAS and isobornyl acrylate (IBA), with ACMAS contents of 10, 25, and 50 wt %, respectively. It can be seen that the silicone (which appears dark in the micrographs) forms a continuous phase, even at silicone contents as low as 10%, while the isobornyl acrylate appears to form spherical microdomains. The scale of the phase separated structure is reduced, and becomes more uniform, as the amount of silicone is increased. At 10% 50K ACMAS, the diameter of the acrylate domains ranges from about 0.1 to 3 microns, and the film is white. At 25% 50K ACMAS the diameter of the acrylate domains is more uniform at about 0.4 microns, and the film becomes somewhat more translucent. Finally, at 50% ACMAS the diameter of the acrylate domains is quite uniform at about 0.1 microns, and the film is fairly clear, exhibiting a bluish tint. At 10% 50K ACMAS the film is a brittle plastic, while at 25% 50K ACMAS the film is a

flexible plastic exhibiting a yield point (with whitening and elastomeric behavior above the yield point), and at 50% 50K ACMAS the film is entirely elastomeric. At low silicone contents, the acrylate spheres are nearly close packed, with very thin silicone regions between the high T_g acrylate spheres. Therefore, significant deformation of the film results in microvoids being created, leading to a plastic-like behavior. As the silicone content is increased, it imparts more of its elastomeric character to the network. The yielding and whitening of the network containing 25% 50K ACMAS will be more fully explored in subsequent sections of this article.

Figure 2(d)–(f) shows electron micrographs of networks comprised of 30K MAUS and IBA, with MAUS contents of 5, 15, and 25 wt %, respectively. At 5% MAUS the silicone forms discrete phases in the acrylate matrix, with the silicone phases ranging from about 0.015 microns to about 0.3 microns in size. As the MAUS content is increased to 15%, the silicone is seen to form a more continuous phase, and at 25% MAUS the continuity of the silicone phase is readily apparent. This change in the continuity of the silicone phase strongly affects the oxygen permeability of the networks, as discussed in a later section. Note that the scale of the phase separation for the network containing 25% 30K MAUS (roughly 0.1 to 0.15 microns), is smaller than that of the corresponding network prepared with 25% 50K ACMAS, due in part to the lower molecular weight of the 30K MAUS. Also, the acrylate phase appears to be more continuous for networks made with 30K MAUS (i.e., bicontinuous structure) compared to networks made with 50K ACMAS. The fact that the methacrylate group of MAUS can undergo copolymerization with growing polyacrylates chain faster than it homopolymerizes might also be contributing to the more uniform, smaller scale distribution of the components. The greater copolymerization rate of the MAUS end groups could also be contributing to the formation of a more bicontinuous phase separated structure. Acrylamide groups of ACMAS, on the other hand, may homopolymerize faster, establishing a continuous silicone network structure at the early stage of polymerization, thus forcing the acrylate monomer to homopolymerize within the already established polysiloxane network. The role that the relative rates of copolymerization vs. homopolymerization play in determining the structure and properties of the networks will be further discussed in a subsequent section of this article.

Figure 3(a)–(c) and Figure 2(b) show electron micrographs of networks comprised of 25% 50K reactive silicone and 75% IBA, with the reactive silicone being MACMAS, MAUS, MeStUS, or ACMAS, respectively. The silicone phase appears to be continuous in all cases. In the case of networks made with MACMAS and ACMAS, the acrylate portion appears to form discrete spherical domains. The network containing MACMAS exhibits the largest scale of phase separation, with the acrylate domain diameter ranging from about 0.5 to 1.2 microns, while the acrylate domains are about 0.4 microns in diameter for the network made with ACMAS. Both of these networks are translucent to white. Networks made with MAUS and MeStUS have a smaller scale of phase separation, on the order of 0.1 to 0.15 microns, and are, therefore, more clear. In addition, the acrylate phases in networks made with MAUS and MeStUs appear to exhibit some continuity (i.e., a bicontinous structure is formed), which would account for the more plastic character of these samples (see Table I).

Similarly, Figure 3(d)–(f) and Figure 2(c) show electron micrographs of networks comprised of 50% 50K reactive silicone and 50% IBA, with the reactive silicone being MACMAS, MAUS, MeStUS, or ACMAS respectively. The silicone phase appears to be continuous and the acrylate phases appear discrete in the cases of MACMAS, MAUS, and ACMAS. The networks made with ACMAS and MACMAS are entirely elastomeric in nature. In contrast, the network made with MAUS behaves in a plastic-like manner at low elongation, but becomes elastomeric after a small degree of deformation. Therefore, there may be some degree of continuity to the acrylate phases in the case of MAUS. The network containing 50K MeStUS exhibits a more irregular morphology, and it is difficult to say which components are continuous. Because the network made with MeStUS exhibits plastic properties, with some elasticity beyond the yield point, it would appear that a bicontinuous structure is present. The scale of the phase separation generally decreases as the reactive silicone content is increased from 25 to 50%. For copolymeric networks having 50% IBA, the scale of the phase separation is fairly similar for the networks containing ACMAS, MACMAS, and MAUS (about 0.1 micron), but much smaller (about 0.01 micron) for the network made with MeStUS. The scale of phase separation is small enough that fairly clear or slightly bluish films are obtained in all cases.

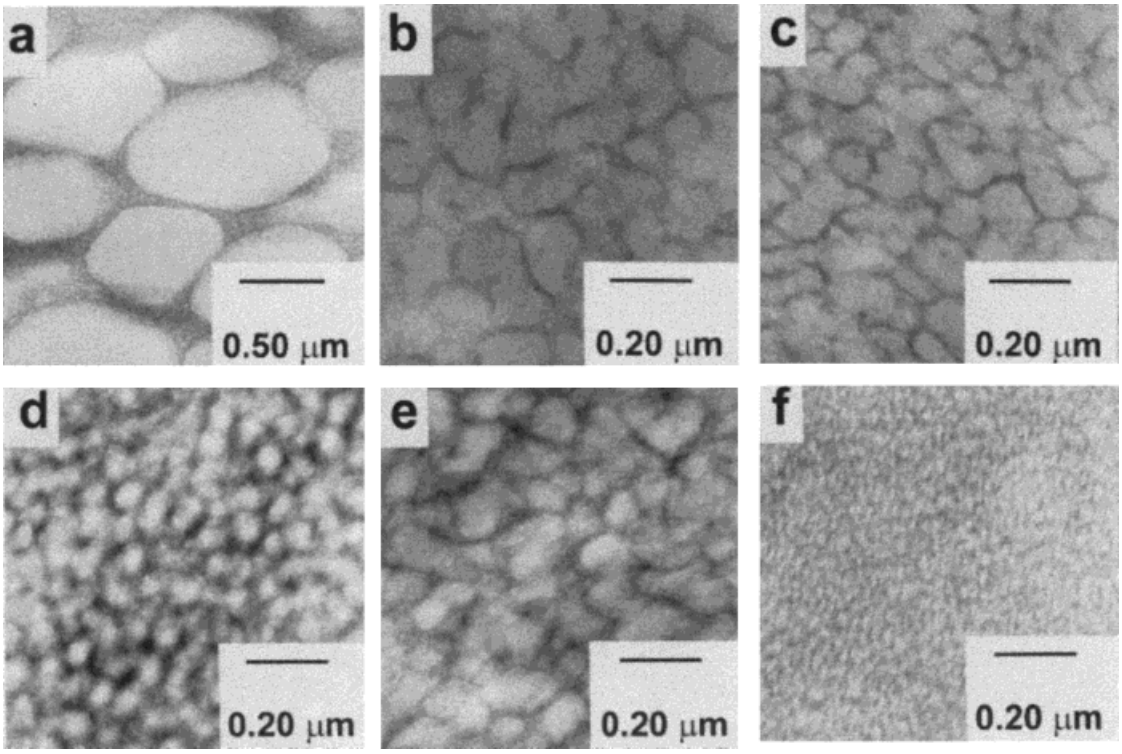

Figure 3 TEMs illustrating the effect of the telechelic siloxane end group on the phase-separated morphology of 25/75 (w/w) 50K siloxane/IBA networks: (a) MACMAS, (b) MAUS, and (c) MeStUS, and 50/50 (w/w) 50K siloxane/IBA networks: (d) MACMAS, (e) MAUS, and (f) MeStUS.

Effect of Reactive Silicone Molecular Weight

Figures 4(a)–(c), 2(b), and 14(a) show electron micrographs of silicone–acrylate networks comprised of 25% ACMAS and 75% IBA, with the ACMAS molecular weight being 5K, 10K, 20K, 50K, and 90K, respectively. In the case of 5K ACMAS, the silicone segments form small discrete domains on the order of 0.01 microns, uniformly distributed throughout the poly-IBA matrix. This finding suggests that, in the solution of 5K ACMAS in IBA monomer, the functionalized silicone may be associated to form discrete clusters (micelles), and that homopolymerization of the ACMAS silicone might take place at the early stage of the free radical polymerization**.** For the network with 10K ACMAS, the silicone phases start to aggregate and form a much larger scale phase separated structure, on the order of 0.5 microns, wherein the silicone is starting to form a somewhat continuous phase. As the ACMAS molecular weight is increased even further, the continuity of the silicone phase becomes more developed, and the IBA portion appears to form discrete spherical domains, with a diameter of about

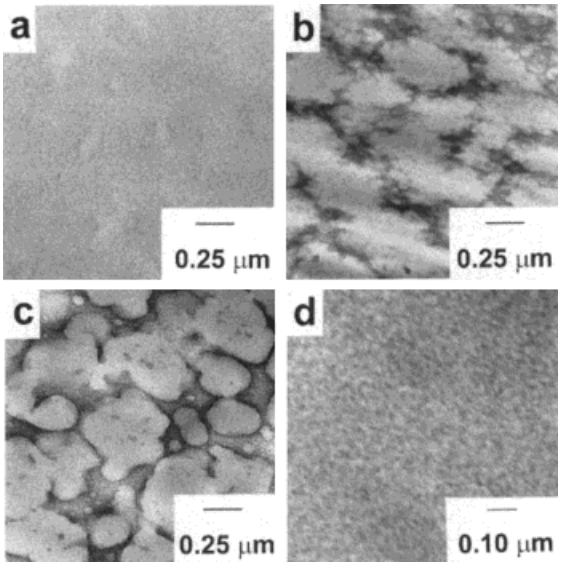

Figure 4 TEMs illustrating the effect of the functional siloxane molecular weight on the phase separated morphology of 25/75 (w/w) ACMAS/IBA networks: (a) 5K, (b) 10K, and (c) 20K, and 25/75 (w/w) 20K MeStUS/IBA network: (d).

0.5 microns, in the silicone matrix. As the ACMAS molecular weight is increased from 5K through 90K, the mechanical response of the networks changes appreciably. At the lower ACMAS molecular weights the networks exhibit a plastic character, while at the higher ACMAS molecular weights (20K and above) the networks whiten and become elastomeric after a small initial deformation. We attribute the whitening to microcavitation (to be discussed later) caused by the inability of the high T_g acrylate domains to deform, or to move without the formation of additional volume. Similar trends were found for networks prepared with MACMAS.

In the case of networks made with MAUS, the continuity of the acrylate phase is maintained even at high MW of functional siloxanes providing the networks with plastic characteristics in the whole range of molecular weights. For instance, the network containing 25% 90K MAUS is a clear plastic material that becomes white when elongated, and does not recover its original shape at room temperature. Only when heated to about 100°C (i.e., above the poly isobornyl acrylate T_g) can it recover its original shape and appearance.

In the case of MeStUS, larger molecular weights are needed before a well-defined continuous silicone phase develops. For example, Figures 4(d) and 3(c) show electron micrographs of networks made with 25% MeStUS and 75% IBA, with the MeStUS molecular weight being 20K and 50K, respectively. In the case of 20K MeStUS, a very fine scale (0.01 to 0.02 microns) irregular phase-separated morphology is observed. Only when the MeStUS molecular weight is increased to 50K does a well-defined continuous silicone phase start to develop. However, even at the higher MeStUS molecular weights, it appears that the polyacrylate phase still retains continuity. This continuity of the acrylate phase dominates the mechanical properties of such networks, as the samples are actually so rigid that they cannot be tested using the Instron method described earlier, breaking easily at low elongation, and whitening upon bending.

Effect of the Choice of Acrylate Comonomer

Figures 2(c), 5(a), and 5(b) show electron micrographs of silicone–acrylate networks comprised of 50% 50K ACMAS and 50% comonomer, with the comonomer being IBA, *t*-butyl acrylate, and methacrylic acid, respectively. In the case of *t*-butyl acrylate, the morphology of the network is fairly similar to that observed earlier in the case of IBA. A continuous silicone phase and discrete acrylate phases are observed, with the scale of the phase separation being about 0.1 to 0.15 microns, resulting in a slightly bluish film which shows good elastomeric properties. However, for the network prepared with methacrylic acid, a more irregular and larger scale phase separated morphology is seen, resulting in a white film. In addition, the network prepared with methacrylic acid is a stiff plastic, indicating that the acrylate component forms a continuous phase.

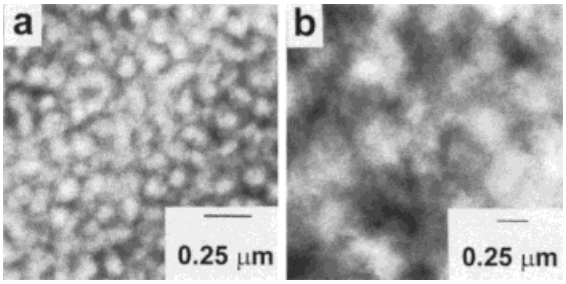

Figure 5 TEMs illustrating the effect of the acrylate monomer on the phase-separated morphology of 50/50 (w/w) 50K ACMAS/acrylate networks: (a) *t*-butyl acrylate, and (b) methacrylic acid.

Mechanical Properties

Effect of Silicone/Acrylate Ratio

Table II summarizes the results of the stress–strain measurements for a series of materials made of 50K ACMAS/IBA at different ratios of the two components. The tensile modulus increases from a characteristically low value of 0.3 MPa for an unfilled silicone elastomer, through the intermediate values typical of filled silicone elastomers, to the very high values more typical of plastic materials (tens of MPa). The data can easily be interpreted in terms of the morphology changes observed by TEM. At a low concentration of the acrylate component, discrete plastic domains are present that can act to reinforce the silicone elastomer. Increasing the concentration of the acrylate component results in steadily increasing tensile moduli and stress at break. At an acrylate concentration higher than about 60%, the tensile modulus increases strongly, and plastic behavior (a yield point) is detectable during the stress–strain measurements. At strains higher than the yield point, the networks exhibit an elastomeric region, with characteristic reversible whitening of the sample. Another observation

Table II Effect of Siloxane/Acrylate Ratio on the Mechanical Properties of 50 K ACMAS/IBA

Siloxane/ Acrylate w/w	Tensile Modulus (MPa)	Stress at Break (MPa)	Strain at Break (%)	Features	Swelling %	Extract. %
100/0	0.3	0.7	390	elastomer	352	6.1
90/10	0.4	0.9	380	elastomer	403	7.2
75/25	1.0	3.9	500	elastomer	415	6.9
60/40	1.6	6.0	390	elastomer, wavy curve	437	7.7
50/50 hiUV	3.4	10.3	340	elastomer, wavy curve	493	7.8
50/50	2.6	8.6	340	elastomer, wavy curve	—	—
40/60	4.0	6.8	210	"yield" at 70–140% elongation	591	7.9
38/62 hiUV	9.1	8.3	190	"yield" at 40–120% elongation	—	—
35/65	7.7	5.6	170	"yield" at 20–60% elongation	644	8.5
30/70	15.1	4.5	100	"yield" at 15–40% elongation	722	9.0
25/75 hiUV	28.4	10.3	110	"yield" at 15–45% elongation	816	9.6

with such networks is that their stress–strain curves can exhibit a slightly "wavy" character (see Figs. 6 and 8) at higher elongations, for acrylate concentrations as low as 40%. A possible interpretation of this phenomenon will be discussed later.

Figure 6 shows some representative stress–strain curves for a series of 35K ACMAS/IBA samples. At 75% acrylate, the elastomeric behavior can only be observed after the sample goes through the "yield point," where the sample changes its appearance from translucent to white. This sample exhibits the morphology of almost close packed hard discrete domains [see Fig. 2(b)]. We attribute the whitening, upon elongation, to microcavitation due to the inability of the glassy acrylate domains to deform, or move freely within the elastomeric matrix, as discussed later. At 62% acrylate the network shows fairly regular elastomeric stress–strain curve at low elongation, but undergoes "yielding" at higher elongations to be followed again by elastomeric behavior at large strains. In the "yielding" zone the sample, originally slightly bluish, becomes white. Again, the whitening is attributed to microcavitation at the yield point. At 50% acrylate, a stress–strain curve more typical of an elastomer is seen, with no yield point observed. Nevertheless, some small deviations of the stress–strain curve from perfect elastomeric behavior can even be observed at 50/50 ratios at higher (150% strain) elongations.

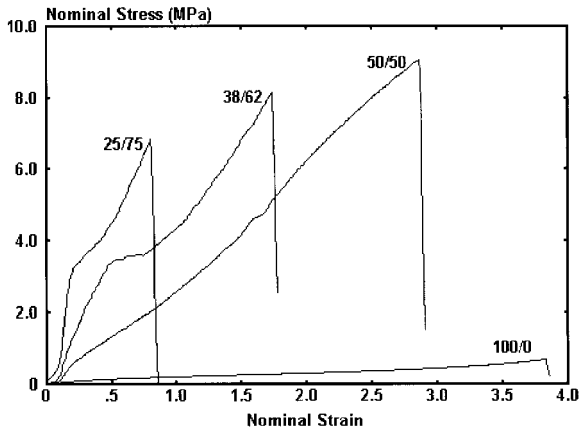

Figure 6 Stress–strain curves of 35K ACMAS/IBA networks at siloxane/acrylate ratios of 100/0, 50/50, 38/62, and 25/75 (w/w).

As shown by the data in Table II, the degree of swellability of the networks increases with decreasing amount of difunctional siloxane. This is expected, because the difunctional siloxane acts as a high molecular weight crosslinker. The amount of extractable material does not increase significantly with increasing acrylate content (over the level observed for the network formed of the silicone itself), indicating that the components of the networks remain chemically bound, and that there is a high degree of conversion of the acrylate monomers. Similar trends have been observed for networks prepared with the other functional siloxanes and acrylates.

Effect of Siloxane Functional Group

The data in Table III and the stress–strain curves illustrated in Figure 7 demonstrate the remarkable differences in the mechanical properties of the copolymeric networks due to the nature of functional siloxane end groups. At both the 25/75 and 50/50 ratio of 50K siloxane to acrylate, two

Table III Effect of Siloxane Functional Group on the Mechanical Properties of 50 K Siloxane/IBA Networks at 25/75 and 50/50 Weight Ratios

Siloxane	Siloxane/Acrylate (w/w)	Tensile Modulus (MPa)	Stress at Break (MPa)	Strain at Break (%)
50 K MeStUS	25/75	[a]	[a]	[a]
50 K MAUS	25/75	60.0	5.7	60
50 K MACMAS	25/75	26.3	8.4	104
50 K ACMAS	25/75	28.4	10.3	112
50 K MeStUS	50/50	20	4.2	380
50 K MAUS	50/50	16	7.1	390
50 K MACMAS	50/50	4.4	10.3	330
50 K ACMAS	50/50	3.4	9.1	340

[a] Not able to test, too brittle.

distinct types of mechanical behavior are seen, depending on the reactive siloxane end group. Networks containing ACMAS and MACMAS form polymers with elastomeric characteristics at the 50/50 ratio. In contrast, networks containing MAUS and MeStUS form plastic materials at the 50/50 ratio, which show elasticity at elongations beyond the yield point. At the 25/75 ratio, networks containing ACMAS and MACMAS form translucent flexible plastics, which whiten (from cavitation) and become elastomeric upon stretching. However, the whitening disappears immediately upon releasing the stress. In contrast, the MAUS, and especially the MeStUS, based materials are high modulus plastics, which whiten irreversibly (at room temperature) upon stretching or bending. These differences in mechanical properties are not surprising in view of their morphological differences observed by TEM (compare Figs. 3(a) through (c) and 2(b) for 25/75 ratios, and Figs. 3(d) through (f) and 2(c) for the 50/50 ratios). ACMAS and MACMAS exhibit a more pronounced continuous silicone phase with the acrylate domains remaining primarily discrete. In the case of MAUS, and especially MeStUS, the acrylate phase remains somewhat continuous, even as the silicone phase gains continuity. This continuity of the acrylate phase must be broken upon elongation at yield point to restore the elastomeric character of continuous silicone network.

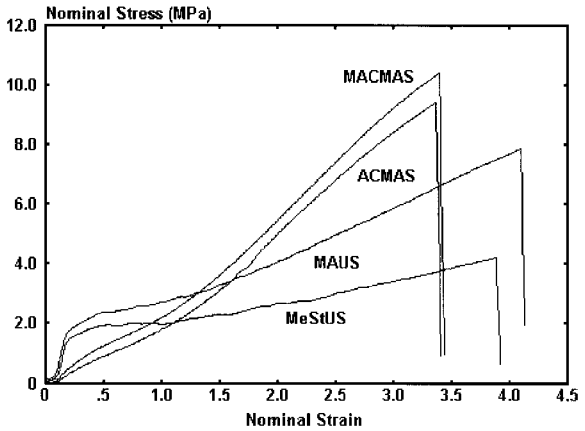

Figure 7 Stress–strain curves of 50/50 (w/w) 50K siloxane/IBA networks vs. siloxane functional end groups: ACMAS, MACMAS, MAUS, and MeStUS.

Effect of the Functional Siloxane Molecular Weight

Table IV lists the stress–strain properties of siloxane–acrylate networks made from a 50/50 ratio of functional siloxane/IBA, as a function of the siloxane molecular weight. In addition, representative stress–strain curves of the series of networks made with ACMAS and MAUS siloxanes are shown in Figures 8 and 9, respectively. While there are similarities in the values of stress at break and the strain at break in the ACMAS and MAUS series, the corresponding materials differ substantially in terms of tensile moduli. The actual stress–strain curves reveal significant differences between the corresponding members of the ACMAS and MAUS families. The networks made of ACMAS show fairly typical elastomeric behavior, with relatively low moduli, down to a molecular weight of 20K. However, in the case of 10K, and especially 5K, the moduli increase markedly, and a distinct bend (pseudo-yield point) in the stress–strain curve is seen at fairly low elongations. For the MAUS series, on the other hand, plastic behavior and high moduli of the samples are observed for all molecular weights.

Table IV Effect of Telechelic Siloxane Molecular Weight on the Stress–Strain Properties of Siloxane–Acrylate Networks, at 50/50 Siloxane/Acrylate Weight Ratio

Siloxane		Acrylate	Tensile Modulus (MPa)	Stress at Break (MPa)	Strain at Break (%)
5 K	ACMAS	IBA	47.7	7.5	120
10 K	ACMAS	IBA	35.6	10.1	210
20 K	ACMAS	IBA	7.3	10.2	240
35 K	ACMAS	IBA	5.3	9.1	300
50 K	ACMAS	IBA	3.4	9.1	340
100 K	ACMAS	IBA	2.1	9.0	350
5 K	MAUS	IBA	66.7	10.1	140
10 K	MAUS	IBA	44.4	10.3	230
20 K	MAUS	IBA	51.0	10.6	310
35 K	MAUS	IBA	32.0	8.9	380
50 K	MAUS	IBA	20.0	7.1	390
20 K	MeStUS	IBA	27.3	5.4	240
35 K	MeStUS	IBA	40.0	7.4	370
50 K	MeStUS	IBA	40.0	7.2	190
100 K	MeStUS	IBA	93.3	6.0	540
35 K	MACMAS	IBA	6.7	8.2	280
50 K	MACMAS	IBA	4.4	10.3	330

The stress–strain data correlate well with the findings of the morphology studies. In the case of networks made with higher molecular weight ACMAS, the discrete plastic domains are surrounded by the continuous silicone (elastomeric) phase [e.g., Fig. 2(b) and (c)], while networks made with MAUS [e.g., Figs. 3(e) and 2(f)] tend to have a more bicontinuous structure. Therefore, the networks made with MAUS behave like plastic materials at low deformations. When the continuity of plastic domains is disrupted (at the yield point) the elastomeric character of the silicone phase is able to dominate the material behavior (i.e., at higher strains). As can be seen in Table IV, networks made with high molecular weight MACMAS exhibit stress–strain properties similar to that of the ACMAS based network. This is not unexpected, considering that the corresponding samples made of ACMAS and MACMAS have similar morphologies [compare Figs. 2(c) and 3(d)]. The mechanical properties of the MeStUS based copolymeric networks more closely

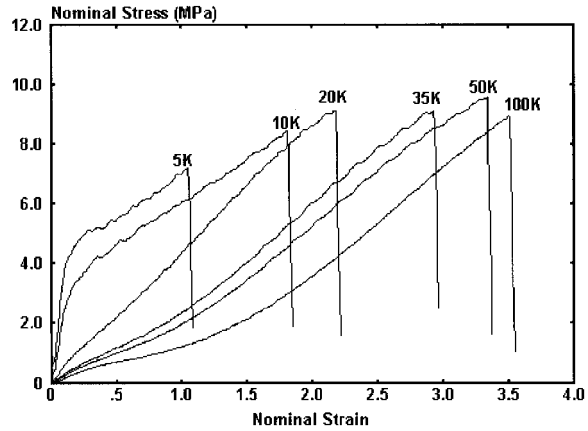

Figure 8 Stress–strain curves of 50/50 (w/w) ACMAS/IBA networks at ACMAS molecular weights of 5K, 10K, 20K, 35K, 50K, and 100K.

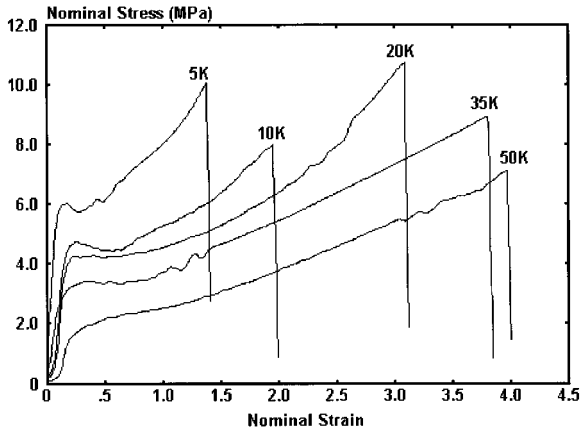

Figure 9 Stress–strain curves of 50/50 (w/w) MAUS/IBA networks at MAUS molecular weights of 5K, 10K, 20K, 35K, and 50K.

Table V Mechanical Properties of Copolymer Networks Made with Mixtures of Functional Siloxanes

Siloxane	Siloxane w/w	Acrylate	Tensile Modulus (MPa)	Stress at Break (MPa)	Strain at Break (%)
50 K	ACMAS/MAUS 50/50	IBA	5.2	6.7	275
25 K	ACMAS/MeStUS 50/50	IBA	26.7	7.9	330
35 K	ACMAS/MACMAS 50/50	IBA	6.3	10.1	310

resemble those of the networks made with MAUS. Networks made with MeStUS form high modulus plastics when copolymerized at a 50/50 ratio with IBA, over the whole range of MeStUS molecular weights. Again, these findings are consistent with the network morphologies observed by TEM. In the case of MAUS, and especially with MeStUS, the morphology appears to be somewhat bicontinuous [Fig. 3(e) and (f), respectively].

Table V lists the stress–strain properties of networks prepared from 50/50 mixtures of functional silicones with IBA, wherein a mixture of two functional silicones were used (at a ratio of 1 : 1). When a mixture of 50/50 50K ACMAS/50K MAUS was used, the resulting stress–strain curve resembled that of a pure ACMAS/IBA network, with a slightly higher modulus. ACMAS could presumably homopolymerize first establishing the continuity of silicone phase and only then the copolymerization of MAUS with IBA would proceed. On the other hand, a network in which a mixture of 35K ACMAS/MeStUS was used had plastic properties with modulus in the range intermediate between the sample made of pure ACMAS and pure MeStUS. A network made from a mixture of 35K ACMAS and MACMAS had properties similar to those made of either component.

Effect of Acrylate Monomer

Table VI lists the characteristics of siloxane–acrylate networks made with *t*-BuA as the acrylate monomer. The networks prepared with *t*-BuA and different molecular weight ACMAS have mechanical properties similar to the corresponding networks made using IBA as the acrylate monomer (see Table IV). The only significant difference being in tensile moduli—lower T_g poly-*t*-BuA gives materials with lower tensile moduli. These findings are consistent with the similar phase separated morphologies observed for the IBA and *t*-BuA containing networks based on ACMAS [see Figs. 2(c) and 5(a)]. In contrast, a significant difference in mechanical response was noticed for the network made of 50% 50K MAUS copolymerized with *t*-BuA compared to the corresponding network made with IBA. The network made with *t*-BuA shows a low tensile modulus and elastomeric character, while the network made with IBA exhibited a much higher tensile modulus and more plastic-like behavior. This difference might be due to the fact that the *t*-BuA monomer polymerizes to a lower T_g polymer. The T_g of the poly-*t*-BuA phase is about 50°C, while that of the poly IBA phase is about 87°C, as judged by the location of the tan delta maximum seen in the

Table VI Characteristics of Siloxane/Acrylate Networks Made with *t*-BuA

Siloxane	Siloxane/ *t*-BuA w/w	Tensile Modulus (MPa)	Stress at Break (MPa)	Strain at Break (%)	Features
5 K ACMAS	50/50	13.9	6.9	230	plastic, yields, tensilizes
10 K ACMAS	50/50	16.5	6.5	260	plastic, yields, tensilizes
20 K ACMAS	50/50	2.4	7.7	230	wavy, elastomer
35 K ACMAS	50/50	1.7	7.5	270	elastomer, slightly wavy
50 K ACMAS	50/50	1.7	8.3	290	elastomer, slightly wavy
100 K ACMAS	50/50	1.7	8.9	410	elastomer, wavy
90 K ACMAS	38/62	3.4	7.8	280	elastomer, "yields" at high elongation, tensilizes
50 K MAUS	50/50	3.1	7.4	420	elastomer
50 K MAUS	25/75	44.4	7.9	140	plastic, yields, tensilizes

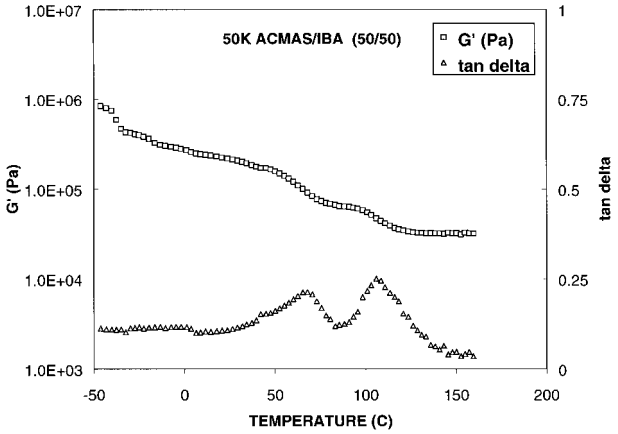

Figure 10 Dynamic-mechanical data for 50/50 (w/w) 50K ACMAS/IBA network. $\nu = 1$ Hz.

dynamic mechanical data of these networks (discussed in the next section, and presented in Figs. 11 and 12). The softer poly-*t*-BuA may show more mobility at the polymerization temperature, and may be able to develop more discrete polyacrylate domains. No morphological analysis by TEM has been performed to confirm this hypothesis, however. The difference in properties between the networks based on IBA vs. *t*-BuA are even more pronounced at higher acrylate concentrations. For example, networks based on 25/75 (w/w) 50K MAUS/IBA form a rather stiff plastic material, which whitens irreversibly when stretched (at room temperature), breaking at only 60% elongation. Its analog, made with *t*-BuA, is somewhat softer, and also whitens when elongated (cavitation); however, the whitening is reversible, although the recovery is rather slow at room temperature.

Dynamic-Mechanical Properties

Dynamic-mechanical properties of films made of 50K ACMAS/IBA (50/50) and 50K MAUS/IBA (50/50) were investigated, with the results shown in Figures 10 and 11, respectively. Recall that these materials, which differ only in the siloxane end group, have different morphologies. The network made with MAUS exhibited somewhat more continuity in the acrylate phase. Also, their corresponding mechanical properties are quite different, the former is an elastomer, while the latter, showed plastic characteristics at small elongation. Dynamic mechanical studies confirm that at 20°C (1 Hz), 50K ACMAS/IBA (50/50) has a shear storage modulus, G', of 2.4×10^5 Pa vs 1.5 $\times 10^7$ Pa for 50K MAUS/IBA (50/50). Even stronger differences were observed in the corresponding loss moduli ($G'' = 2.5 \times 10^4$ Pa vs 4.0×10^6 Pa, respectively). The storage modulus vs. temperature scan of the ACMAS-containing sample shows the first transition at about −40°C, which can be attributed to the melting of the crystalline siloxane component, followed by a gradual decrease of the modulus, with two more transitions observed at temperatures of about 65 and 105°C. These higher temperature transitions are both thought to be due to the T_gs of the polyisobornyl acrylate component, either polymerized within the already phase separated acrylate domains or polymerized while still mixed with the siloxane segments. Note that the level of G' does not change much on going through these higher temperature transitions, indicating that the siloxane component is dominating the mechanical response at small deformations (due to the discrete nature of the acrylate phases).

In contrast, the network made of 50K MAUS/IBA (50/50) appeared to have a more bicontinuous morphology, as evidenced by TEM and stress–strain measurements. Thus, the plastic character of poly IBA phase should dominate the properties of the network below the T_g of the poly IBA. At temperatures above the T_g of the poly IBA phase, the continuous siloxane phase should play a more important role. Indeed, although in the range from 0°C to the onset of poly IBA glass transition, the storage modulus is observed to decrease somewhat, (possibly due to changes in the phase mixing in the interphase regions) it is only in the temperature range between 70–90°C (max tan δ ~87°C), that a steep transition in G' is observed,

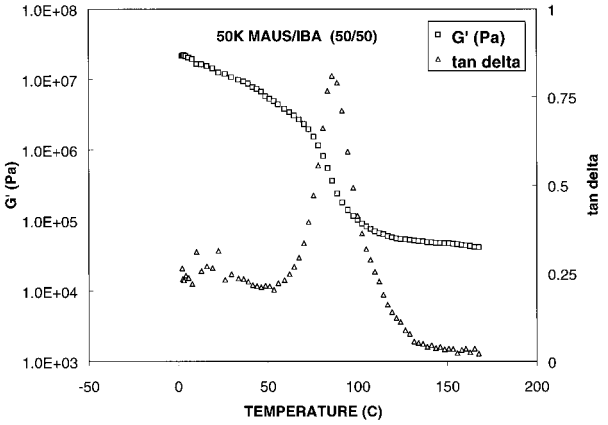

Figure 11 Dynamic-mechanical data for 50/50 (w/w) 50K MAUS/IBA network. $\nu = 1$ Hz.

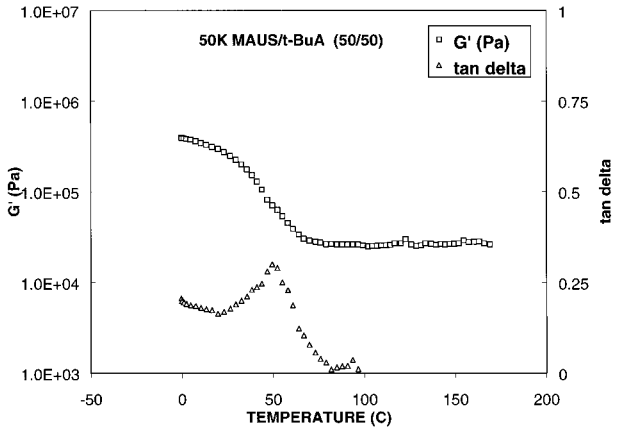

Figure 12 Dynamic-mechanical data for 50/50 (w/w) 50K MAUS/*t*-BuA network. $\nu = 1$ Hz.

followed by a fairly steady plateau up to at least 180°C.

The dynamic-mechanical scans of 50K MAUS/*t*-BuA (50/50) are shown in Figure 12. The general appearance of the scans is similar to those of 50K MAUS/IBA (50/50). However, note that the T_g transition of the poly-*t*-BuA phase is observed at a lower temperature range of 40–60°C (max tan δ ~50°C) compared to that of the poly IBA phase. Another difference is that the storage modulus for the *t*-BuA containing network, at temperatures below the acrylate T_g, are significantly lower than the corresponding network made with IBA. As described earlier, the network made with *t*-BuA showed elastomeric character during stress–strain testing at room temperature. For these MAUS based materials, both the dynamic mechanical and stress–strain testing point to a morphology of discrete acrylate domains in the case of *t*-BuA and acrylate phase continuity in the case of IBA.

Further Deformation Studies

Some of the characteristic phenomena associated with the deformation of the siloxane-acrylate networks have already been mentioned. The materials differ greatly in terms of their appearance, as some of them are crystal clear, some have a light bluish tint, some are translucent, and some hazy or white. In the broad family of materials that have been prepared, there are plastics and elastomers. Some of the materials show plastic behavior at small strains, and become elastomeric at higher elongations. The most unusual materials are those that become white upon stretching but reversibly become clear once the stress is released. Characteristic whitening upon stretching was associated in some cases (at high acrylate content), with easy to feel apparent "friction" upon stretching by hand. The working hypothesis was put forward that the whitening was associated with microcavitation taking place at the interfaces between the glassy acrylate domains and the siloxane matrix.

Cold Stretching

To corroborate the hypothesis of microcavitation, networks made of 25% 25K or 35K MAUS and 75% IBA were stretched beyond their yield point at room temperature, and while stretched, irradiated with electron beam to "fix" the structure in place by crosslinking. The morphology of the samples was then determined using TEM. Figure 14(d) shows an electron micrograph of the silicone–acrylate network based on 25K MAUS, after stretching. Long thin cracks (microcavitation) are evident as a result of the stretching. It appears that there are thin siloxane filaments that bridge the cracks. Similar results were seen for the network made with 35K MAUS as the siloxane component.

As a consequence of the microcavitation upon stretching, one would anticipate an increase in the volume of the sample. This increase in volume should be reflected in a Poisson ratio that is lower than that expected for an ideal elastomer (0.5). To study this aspect of the networks' characteristics the deformation of a few select samples was studied. Figure 13 illustrates volume changes upon room temperature elongation for networks containing 90K ACMAS and (a) 50% IBA, (b) 68% *t*-BuA, or (c) 75% IBA. At 50% IBA the discrete high T_g acrylate domains appear to function as an *in situ* filler, providing the film with good elastomeric characteristics. For this network, there is no volume change observed upon stretching, as expected for an ideal elastomer.

Higher concentrations of a high T_g acrylate component (68% *t*-BuA) also provide for significant reinforcement of the elastomer and, up to about 90% elongation, no volume changes are observed. However, as the sample is further stretched it becomes white (cavitation), and the volume of the sample increases linearly upon further stretching up to the break point.

In the case of even higher concentrations of the acrylate component (75% IBA), for which the high T_g acrylate domains are nearly close-packed, the

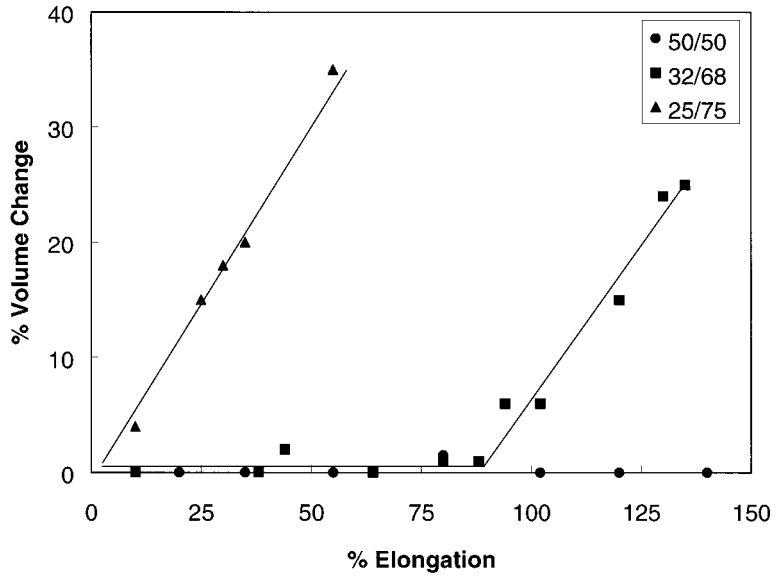

Figure 13 Volume change as a function of elongation for networks comprised of 50/50 (w/w) 90K ACMAS/IBA, 25/75 (w/w) 90K ACMAS/IBA, and 32/68 (w/w) 90K ACMAS/*t*-BuA.

sample increases volume upon stretching, even at low elongation. This is associated with the visual changes observed upon elongation: the film, originally translucent/white, becomes white in the sections that undergo elongation. The elongation of the sample proceeds in zones starting at the ends of the coupon. The data is in good agreement with the stress–strain curve of the sample, which indicated plastic deformation of the sample at low strains. At an elongation of 55%, the Poisson ratio for this sample is only about 0.1.

Hot Stretching

Copolymer networks discussed in this article can be considered as molecular composites in which the glassy domains of high T_g acrylates restrict longer range deformation of the samples. Thus, it was of interest to investigate the behavior of deformed samples upon heating at temperatures above the acrylate T_g, where the acrylate domains are able to deform. Certain copolymeric network materials were submitted to a multistep deformation (see Experimental section) by elongating the sample to near its break point, heating above the acrylate T_g while fixed in a jig, and then cooling the samples under stress (while still in the jig) to quench the acrylate domains in their new arrangements. This deformation cycle could typically be repeated three to five times.

The following general features were noted during these deformation experiments. First of all, even the samples that were hazy and white became more clear once heated and then quenched in the elongated state. Second, once cooled and released from the elongation fixture, the samples show only marginal (a few percent) elastic recovery. Another interesting result was that the fully stretched and cooled samples exhibited a new regime of elastic deformation. As shown in Table VII, the samples could be deformed three to five times to an ultimate elongation of several hundred percent. Following this deformation regime, all samples nearly recovered their original shapes, sizes, optical appearance, and mechanical characteristics upon being heated for 0.5 h at 120°C (with no stress applied).

In some cases the samples were also submitted to deformation at a constant stress (dead-load) at 100–120°C, and subsequently cooled to room temperature while under stress. Similarly to the results described above for the multistep deformation regime, the samples show much higher ultimate elongation than the samples deformed in one step at room temperature. They maintain a highly elongated state when quenched, and show a return to their original shape when heated in the absence of stress. Such a procedure was used to prepare samples for TEM analysis to study the effect of deformation, at temperatures above the polyacrylate T_g, on the morphology. Figure 14(a)–(c) shows electron micrographs of a silicone–acrylate network comprised of 25% 90K ACMAS and

Table VII Multistep Deformation of 90 K MW Siloxanes/Acrylate Networks

Siloxane	Acrylate	Ratio	ε_1	ε_2	ε_3	ε_4	ε_5	ε_0'
ACMAS	IBA	25/75	0.47	1.18	1.76	2.12		0.13
ACMAS	IBA	50/50	1.00	1.85	2.32	2.91	3.33	0.05
ACMAS	*t*-BuA	38/62	1.44	3.25	4.53	5.79		0.03
MeStUS	IBA	50/50	1.80	2.12	3.29			0.08

ε_n = tensile strain after nth stretching cycle.
ε_0' = residual tensile strain after heating to 120°C for 0.5 h (with no stress applied).

75% IBA. Figure 14(a) shows that in the undeformed state the IBA forms discrete spherical domains, about 0.5 to 0.6 microns in diameter, with the silicone forming the continuous phase. This network was heated to 120°C (i.e., above the T_g of the IBA phases) and then elongated approximately 200%. The sample was quenched while stretched, and then examined by TEM. Figure 14(b) shows a view of the morphology perpendicular to the stretch direction. The stretching direction was along a 45 degree angle (from lower left to upper right) in the micrograph. The IBA spheres present in the undeformed sample are seen to form ellipses upon stretching, with the long axis in the direction of the stretching. The long axes of the ellipses are about 1.2 microns in length, roughly double that of the original diameter of the spherical domains. Figure 14(c) is a view along the direction of the stretching. Note the reduction in the cross-sectional area of the IBA domains upon stretching. Notably, the sample, originally translucent/white, became almost clear upon heating under stress and remained clear until it was heated again (no stress) to recover its original shape and appearance. This change in optical appearance is attributed to the changing shape and size of the acrylate domains upon deformation. Samples heated, biaxially stretched, and cooled while stretched should give films with disk-like hard acrylate domains. The films should demonstrate heat shrinkability in the x-y plane with heat expansion in the z-direction. No experimental evidence for this effect has been sought, however.

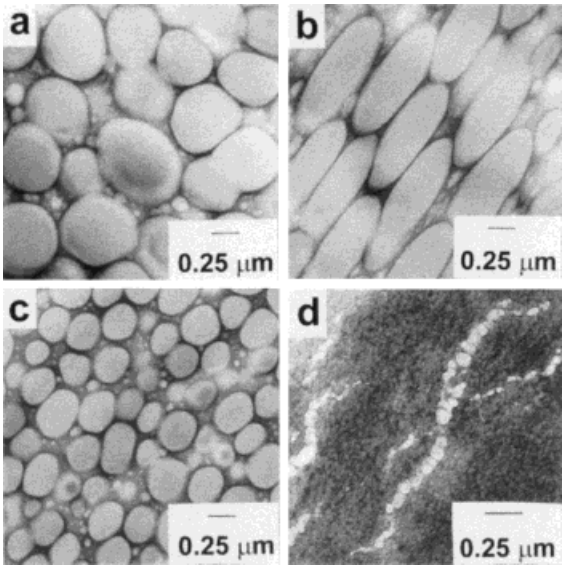

Figure 14 TEMs illustrating the effect of high-temperature deformation on the phase-separated morphology of 25/75 (w/w) 90K ACMAS/IBA: (a) undeformed sample, (b) a view perpendicular to the stretch direction, and (c) a view along the stretch direction. Micrograph (d) shows the microcavitation, which developed for a 25/75 (w/w) 25K MAUS/IBA network upon cold stretching beyond the yield point.

Oxygen Permeability of Siloxane–Acrylate Networks

The oxygen permeability of a series of siloxane–acrylate networks comprised of 30K MAUS and IBA was measured to assess the influence of the phase-separated morphology on transport properties. Networks having 0, 5, 15, 30, 70, and 100% 30K MAUS were used for this study. As shown earlier in Figure 2(d)–(f), the silicone phase develops some degree of continuity at 30K MAUS contents as low as 15%. (In some cases illustrated earlier, for example, for high molecular weight ACMAS/IBA systems, the continuity of silicone phase is evident at silicone concentrations as low as 10%). Because the oxygen permeability of the elastomeric silicone component is expected to be orders of magnitude larger than that of the glassy IBA component, the continuity of the silicone phase is expected to have a large influence on the oxygen permeability of the copolymer network.

The oxygen permeability was measured using a MOCON oxygen permeability tester. The re-

Table VIII Oxygen Permeability of Siloxane/ Acrylate Copolymer Networks

Network Composition (% by Weight)	Oxygen Permeability (cm^3_{STP} cm/m^2 day atm)	(Barrer)
IBA	15.5	2.37
30 K MAUS/IBA 5/95	15.9	2.43
30 K MAUS/IBA 15/85	122	18.6
30 K MAUS/IBA 30/70	666	102
30 K MAUS/IBA 70/30	3490	532
30 K MAUS	5240	799

sults are listed in Table VIII, and are also shown graphically in Figure 15, which shows a plot of the log of the oxygen permeability vs. the volume fraction of 30K MAUS in the network. The upper and lower bounds of oxygen permeability, as a function of composition, should be given by the parallel and series laws, respectively[28]

$$P_{\text{parallel}} = P_1\phi_1 + P_2\phi_2$$

$$P_{\text{series}} = P_1P_2/(\phi_1P_2 + \phi_2P_1)$$

where P_1, P_2, ϕ_1, and ϕ_2 refer to the permeability and volume fractions of phases 1 and 2, respectively. These two limits correspond to diffusion parallel and perpendicular to a lamellar structure. For a morphology of spherical domains embedded in a matrix, the permeability of the composite can be written as[28]

$$P = P_m[P_d + 2P_m - 2\phi_d(P_m - P_d)] \div [P_d + 2P_m + \phi_d(P_m - P_d)]$$

where m and d refer to the matrix and the dispersed phase, respectively. The theoretical predictions of the parallel, series, and spherical morphology models are compared to the experimentally determined permeabilities of the 30K MAUS/IBA networks in Figure 15. Note the abrupt increase in oxygen permeability between 5 and 15% MAUS. This is a direct result of the increase in the continuity of the silicone phase, as evidenced by TEM, at MAUS concentrations equal to or greater than about 15%. At the higher MAUS contents the permeability approaches that predicted by the parallel model, consistent with the observed continuity of the silicone phase.

Polymerization Scenario

The scenario envisioned during the network formation is as follows. Originally, the siloxane chains are dissolved in the acrylic monomers (and photoinitiator). Due to their highly polar nature, the siloxane end groups will tend to associate with each other forming a transient network structure in the acrylic monomer. If the volume fraction of siloxane chains in the system is high enough, this siloxane network can fill space uniformly; otherwise isolated siloxane-rich aggregates may be suspended in the acrylic monomers. After irradiation begins, and free radicals are generated, polymerization may proceed at the siloxane endgroup aggregates (silicone homopolymerization), or between acrylic monomers (acrylate homopolymerization), or the crossover reaction between growing acrylic chains and siloxane end groups can also occur (copolymerization). As

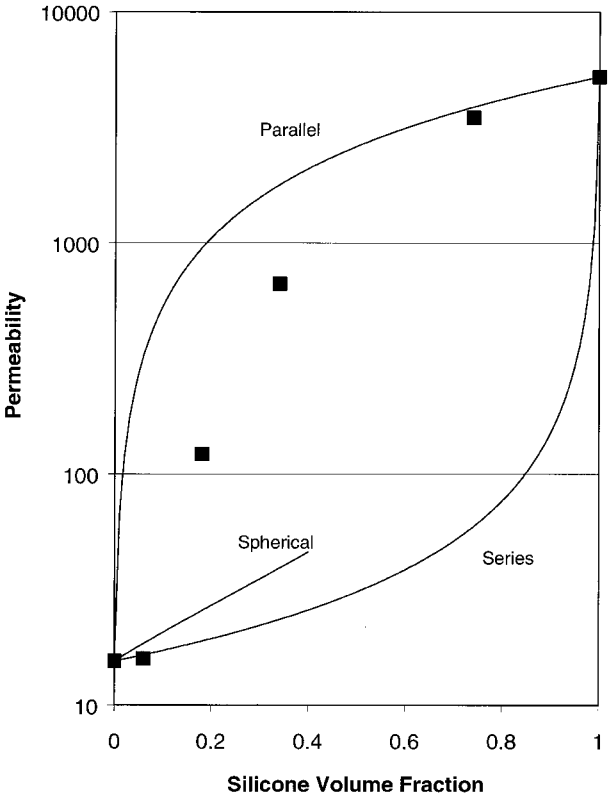

Figure 15 Plot of the log of the oxygen permeability (cm^3_{STP} cm/m^2 day atm) vs. the silicone volume fraction for networks comprised of 30K MAUS and IBA (experimental data points shown as filled squares). The oxygen permeability versus silicone volume fraction predicted based on the series, parallel, and spherical silicone domain morphology models (using the measured pure component permeabilities) are also shown.

polymerization proceeds and the concentration of high molecular weight polyacrylate and polysiloxane components increase, the polysiloxane and polyacrylate components will eventually become incompatible and phase separate, subject to the restrictions imposed by the molecular architecture (e.g., crosslinking sites already formed) of the growing hybrid network. Further polymerization must occur within this phase separated system.

Thus, there are several competing factors that may influence how the polymerization and phase separation proceed in these acrylic-siloxane hybrid networks including: (1) the degree (i.e., strength) of association of the polar siloxane end groups prior to and during the polymerization; (2) the volume fraction of siloxane in the system; (3) the relative rates of siloxane–siloxane, siloxane–acrylate, and acrylate–acrylate reactions; (4) the degree of (in)compatibility between the siloxane chains and the acrylic monomers and, as polymerization proceeds, between the siloxane and polyacrylate chains; and (5) the rate of the different polymerization reactions vs. the rate of phase separation. It was hoped that by studying the resultant morphology the way in which these factors influence the polymerization pattern could be deduced.

An indication of the relative abilities of the different reactive siloxanes to aggregate (i.e., strength of the polar end group association) can be ascertained from their relative viscosities. As the data in Table IX shows, the ACMAS and MeStUS series have a much higher viscosity than the MACMAS and MAUS series, and are therefore expected to be more strongly associated. Of course, the association of the siloxane end groups will also be dependent on the ability of the acrylate monomer to solvate the end groups. More polar (meth)acrylate monomers, such as methacrylic acid, should lead to less association of the siloxane end groups.

The volume fraction of siloxane for which there is a complete filling of space by the swollen transient siloxane network can be considered to be the borderline between systems in which the siloxane forms discrete domains and systems in which the siloxane may form a continuous phase.

The relative abilities of the different functional siloxanes to undergo homopolymerization vs. copolymerization with acrylates is also known. The acrylamide group homopolymerizes easier than it copolymerizes with acrylates while methacrylate end groups undergo somewhat easier copolymerization with acrylates than homopolymerization (crossover reaction between acrylate and methacrylate is favored over the crossover from methacrylate to the acrylate, and over homopolymerization of methacrylates and acrylates). Alpha-methylstyryl groups cannot homopolymerize, and therefore, can only undergo copolymerization with acrylates. This requires that aggregates of the functional endgroups dissociate before any copolymerization reaction can take place. Naturally, each polysiloxane chain-end must be separated from another siloxane end group by the growing polyacrylate chain. Not surprisingly, very small scale phase separation is observed in all MeStUS-based copolymeric networks.

When functional polysiloxanes oligomerize, the process is associated with a dramatic increase in the molecular weight of the polysiloxane molecules. Therefore, the mobility of the polysiloxane molecules would be quickly reduced. If the concentration of polysiloxane is high enough to form a continuous network in the polymerization volume at the early stage of the reaction, by either homo-oligomerization or by partial copolymerization with the acrylate monomer before any major portion of the acrylate monomers is polymerized, the remaining polymerization components would be forced to polymerize within such a pre-formed network. Such might be the situation in the co-

Table IX Viscosities of Telechelic Siloxanes

Siloxane	Molecular Weight	Viscosity at 25°C ($Pa \cdot s \times 10^3$)
Silicone Diamine	5,000	130
	10,000	360
	20,000	1,640
	35,000	7,060
ACMAS	5,000	49,200
	10,000	52,400
	20,000	83,600
	35,000	84,000
MACMAS	5,000	3,300
	10,000	2,500
	20,000	6,100
	35,000	11,300
MAUS	5,000	4,900
	10,000	6,500
	20,000	21,600
	35,000	51,500
MeStUS	5,000	59,200
	10,000	29,400
	20,000	81,600
	35,000	137,000

polymer systems containing a high concentration of functional siloxanes. All of the copolymer networks containing 50% siloxane (except in the case of MMA) are either clear, or bluish, indicating a small scale of phase separation, as the polymerization of the remaining monomers must continue within relatively uniformly distributed constraints of the network. A lower crosslink density of the siloxane network (higher siloxane molecular weight) should, in general, lead to a larger scale of phase separation because the acrylate portion is able to form larger domains. Indeed, more bluish films are seen for networks made with higher molecular weight ACMAS siloxanes. At which stage of the polymerization such preformed networks are formed, either primarily by oligomerization of functional siloxanes, or through their acting as crosslinkers in the copolymerization with acrylates, would depend on the relative reactivities of the functional groups participating in the reaction.

For the sake of qualitative correlation between the morphology and the composition of the copolymeric networks, the following hypothetical mechanisms might be postulated. If the polymerization of functional siloxane end group aggregates is favored, the oligomerization of polysiloxane would quickly lead to gellation. Any acrylate polymer chains initiated at the siloxane end groups would initially grow in intimate contact with polysiloxanes (in the vicinity of the crosslinking sites of the network) forming a mixed interphase region. Subsequent acrylate homopolymerization would lead to the formation of separate polyacrylate domains. Higher concentration of siloxane functional end groups (lower siloxane molecular weights) should lead to larger mixed interphase volume fraction and smaller acrylate domains sizes.

On the other hand, if the polymerization between the acrylate monomers is favored, the homopolyacrylate formed within the swollen transient siloxane network can phase separate and form its own domains, perhaps breaking the continuity of the siloxane phase (particularly easy at low concentration of functional siloxanes), until the growing acrylate chain reacts with siloxane crosslinker, eventually leading to gellation and freezing-in of the network structure. The homopolymerization of acrylate within its own domains may lead to larger acrylate domain sizes, particularly when the probability of reacting with functional siloxanes (crosslinking reaction) is low.

Finally, there is the case where the crossover (copolymerization) reaction between acrylate and siloxane is favored over homopolymerization. In such a case, the growing polymer chain must seek its counterpart to react with, leading to significant phase mixing and a small scale of phase separation. The example of such a system is provided by the copolymerization of MeStUS with acrylate monomers. Not surprisingly, in all of the MeStUS containing systems studied, the materials are clear, and they exhibit a plastic character, suggesting continuity of the acrylate phase.

In all three cases, lower concentrations of functional siloxane endgroups (e.g., through lower siloxane contents or higher siloxane molecular weight) favor the formation of larger and more well-defined discrete acrylate domains. The continuity of the siloxane phase is favored for systems in which the concentration of siloxane is high enough to form a continuous transient network swollen with acrylate monomers. This may not be the case at lower siloxane contents, for example, at 5 wt % of MAUS [see Fig. 2(d)]. However, siloxanes that homopolymerize readily (e.g., ACMAS) are able to form a continuous siloxane phase at low siloxane contents [see Fig. 2(a)].

The continuity of the siloxane phase in the copolymeric networks is the key to the elastomeric properties of the materials. When polyacrylate forms primarily discrete domains within the siloxane network such plastic domains act to reinforce the silicone elastomers, thus providing materials with good elastomeric properties. When the acrylate phase does not form clearly discrete domains, and there might be a considerable degree of phase mixing (such as in the case of lower molecular weight functional siloxanes), the material properties may be dominated, at the least at low deformations, by the plastic character of polyacrylate phases. In most cases, when the continuity of the acrylate phase is broken (beyond the yield point) the materials will behave like elastomers, as the continuous siloxane network will dominate the properties at higher elongations. In the case of networks made with MAUS and MeStUS such a behavior is even characteristic of high molecular weight siloxanes at high siloxane content. Once the continuity of the acrylate phases is broken it is not restored when the stress is released, unless the samples are heated above the T_g of polyacrylate. This is in contrast to the situation in which well-developed discrete acrylate domains are formed (e.g., 25/75 50K ACMAS/IBA and 50K MACMAS/IBA). In these cases the

materials are flexible pseudoplastics. The morphology of the samples is that of large acrylate domains nearly close packed. Filled with such hard spheres the continuous silicone matrix can only provide some flexibility to the material. Elongation of the sample, and the concomitant contraction of the sample in the radial direction, is virtually impossible due to the incompressibility of the rigid close packed acrylate domains, unless internal voids are created within the material. Indeed, upon elongation the network, translucent, or white, becomes whiter than it was before. Clearly visible zones of deformation are observed perpendicular to the direction of stretching. The deformation is accompanied by an easy to feel "friction." Rather remarkably, the whitening disappears as soon as the stress is released. The whitening was proven to be associated with the formation of cavities. Interestingly, similar phenomena were observed in the systems containing lower concentration of polyacrylates (see: 50K ACMAS/IBA 38/62, 35K ACMAS/IBA 38/62, or 90K ACMAS/*t*-BuA 38/62) when samples were deformed to a larger extent. The interpretation of the phenomenon is based on the same principle except that, in this case, the materials are able to be elongated to a small degree before the cavitation occurs. Again, the whitening due to the cavitation is fully reversible as soon as the stress is released.

Interestingly, all of the samples prepared have a high degree of acrylate monomer conversion despite the fact that the polymerizations were conducted at ambient temperatures—much lower than the T_g of polyacrylates formed as a result of the reaction. This suggests that the siloxane may function as a matrix in which high T_g polymer is formed before it phases out to form its own high T_g domains. A similar finding and interpretation has been put forth previously in the literature for other IPN systems.[29,30]

CONCLUSIONS

This article presents a broad class of materials made by copolymerization of a family of telechelic free radically polymerizable siloxanes with various acrylate monomers that polymerize to form high T_g polymers. Films with properties ranging from those characteristic of strong elastomers to plastics have been obtained by UV-initiated bulk copolymerization of functional siloxanes dissolved in acrylate monomers (in the presence of photoinitiator). The molecular weight of the functional siloxanes, the nature of functional end groups, the choice of (meth)acrylate comonomer, and the siloxane/acrylate ratio all have a rather dramatic effect on the morphology, and thus, on the properties of the copolymeric networks. Physical properties of the materials, such as optical appearance and mechanical and transport properties, are correlated with the unique morphologies observed by TEM studies. Unusual properties such as reversible whitening of some of the materials and low Poisson ratios have been attributed to the microcavitation observed when high T_g acrylate domains interfere with the network deformation. Networks composed of high T_g acrylates (major fraction) coreacted with elastomeric siloxanes can provide heat-shrinkable materials when they are elongated at temperatures higher than the T_g of the corresponding polyacrylates and quenched. The scope of the study made it challenging to perform a more in-depth analysis of the correlations between the various parameters determining the morphology of such copolymeric networks; however, some interpretations of the observed phenomena have been proposed.

This article was presented in part at the XIth International Symposium on Organosilicon Chemistry, Montpellier, France, 1996. The authors would like to acknowledge Dr. Mary Buckett for obtaining some of the TEM micrographs. In addition, Jeanie Snell helped to prepare some of the silicone–acrylate copolymer networks, Dr. Robert Galkiewicz assisted with the mechanical property analysis, and Dr. James Sax helped with permeability studies.

REFERENCES

1. Hoffman, J. J.; Leir, C. M. Polym Int 1991, 24, 131.
2. Galkiewicz, R. K.; Kantner, S. S.; Leir C. M.; Mazurek, M. Proc. 33rd IUPAC International Symposium on Macromolecules, Montreal, Canada, July 1990, Session 1.9.5.
3. Mazurek, M.; Kantner, S. S.; Galkiewicz, R. K. Proc. 14th Annual Meeting of the Adhesion Society, Clearwater, FL, Feb. 1991, p. 39.
4. Gent, A. N.; Liu, G.L.; Mazurek, M. J Polym Sci Polym Phys Ed 1994 , 32, 271.
5. Mazurek, M. H.; Kantner, S. S.; Leir, C. M.; Bogaert, Y. A.; Galkiewicz, R. K.; Sherman, A. A. U.S. Pat. #5,091,483 1992.
6. Mazurek, M. H.; Kantner, S. S.; Kinning, D. J.; Bogaert, Y. A. U.S. Pat. #5,514,730 1996.

7. Sperling, L. H.; Sarge, H. D. J Appl Polym Sci 1972, 16, 3041.
8. Ebdon, J. R.; Hourston, D. J.; Klein, P. G. Polymer 1984, 25, 1633.
9. McGarey, B.; Richards, R. W. Polymer 1986, 27, 1315.
10. Ebdon, J. R.; Hourston, D. J.; Klein, P. G. Polymer 1986, 27, 1807.
11. Klein, P. G.; Ebdon, J. R.; Hourston, D. J. Polymer 1988, 29, 1079.
12. Frisch, H. L.; Gebreyes, K.; Frisch, K. C. J Polym Sci Polym Chem Ed 1988, 26, 2589.
13. McGarey, B. In Advances in Interpenetrating Polymer Networks; Klempner, D.; Frisch, K. C., Eds.; Technomic Publishing: Lancaster, PA, 1989, p. 69, vol. I.
14. Hourston, D. J.; Zarandouz, M. In Advances in Interpenetrating Polymer Networks; Klempner, D.; Frisch, K. C., Eds.; Technomic Publishing: Lancaster, PA, 1990, p. 101, vol. II.
15. Xiao, H.; Ping, Z. H.; Xie, J. W.; Yu, T. Y. J Polym Sci Polym Chem Ed 1990, 28, 585.
16. He, X. W.; Widmaier, J. M.; Herz, J. E.; Meyer, G. C. Polymer 1992, 33, 866.
17. Frisch, H. L.; Huang, M. W. In Siloxane Polymers; Clarson, S. J.; Semlyen, J. A. Eds.; Prentice Hall: Englewood Cliffs, NJ, 1993; p. 649.
18. Sperling, H. L. In Interpenetrating Polymer Networks; Klempner, D.; Sperling, L. H.; Utracki, L. A. Eds.; ACS Series 239; American Chemical Society: Washington, DC, 1994, p. 3.
19. Cully, M.; Pines, A. N.; Metzler, R. B.; Babian, G. W. U.S. Pat. #4,201,808 1980.
20. Chromecek, R. C.; Deichert, W. G.; Falcetta, J. J.; VanBuren, M. F. U.S. Pat. #4,276,402 1981.
21. Carter, R. G.; Miller, W. P.; Watson, S. L. U.S. Pat. #4,369,300 1983.
22. Gornowicz, G. A.; Tangney, T. J.; Ziemelis, M. J. U.S. Pat. #4,563,539 1986.
23. Mueller, K. F.; Lohmann, D.; Falk, R. A. U.S. Pat. #4,605,712 1986.
24. Keryk, J. R.; Varaprath, P. J.; Wright, A. P. U.S. Pat. #4,911,986 1990.
25. Lu, P. C. U.S. Pat. #5,425,991 1995.
26. Nguyen, T. V.; Allen, J.; Yu, Q. U.S. Pat. #5,616,629 1997.
27. Yu, X.; Nagarajan, M. R.; Li, C.; Speckhard, T. A.; Cooper, S. L. J Appl Polym Sci 1985, 30, 2115.
28. Hopfenberg, H. B.; Paul, D. R. In Polymer Blends; Paul, D. R.; Newman, S. Eds.; Academic Press: New York, 1978, p. 445, vol. I.
29. Sperling, H. L. In Interpenetrating Polymer Networks; Klempner, D.; Sperling, L. H.; Utracki, L. A. Eds.; ACS Series 239; American Chemical Society: Washington, DC, 1994, p. 29.
30. Jin, S. R.; Windmaier, J. M.; Meyer, G. C. Polymer 1988, 29, 346.